

Phase retrieval for improved three-dimensional velocimetry of dynamic x-ray blood speckle

S. C. Irvine,^{1,a)} D. M. Paganin,¹ S. Dubsky,² R. A. Lewis,³ and A. Fouras⁴

¹School of Physics, Monash University, Victoria 3800, Australia

²Division of Biological Engineering, Monash University, Victoria 3800, Australia

³Monash University Centre for Synchrotron Science, Monash University, Victoria 3800, Australia

⁴Division of Biological Engineering, Monash University, Victoria 3800, Australia

(Received 22 May 2008; accepted 26 September 2008; published online 15 October 2008)

High-resolution synchrotron-based x-ray phase-contrast images of *in vitro* blood flow have been collected. We demonstrate that the application of a single-image phase retrieval algorithm to the images leads to improved detail in particle image velocimetry correlation peaks. Out-of-plane variation in flow has been extracted from the peaks leading to the three-dimensional reconstruction of velocity across an axially symmetric cylinder. © 2008 American Institute of Physics. [DOI: 10.1063/1.3001592]

Mortality and morbidity rates caused by vascular diseases today rank among the world's highest.¹ With the discovery of the link between blood-flow velocity gradients and atherosclerotic growth² it is clear that the study of hemodynamics is of correspondingly high importance. Multidimensional velocity-field measurements of blood flow are mainly limited to ultrasound Doppler techniques, but generally suffer from poor spatial resolution.³ Recently, it has been shown^{4,5} that x-ray particle image velocimetry (x-ray PIV) displays great potential as a tool for opaque flow measurements, even without the need for tracer particles.

PIV involves the statistical analysis of displacement between consecutive pairs of images of tracer particles taken a small time apart. It is traditionally implemented using visible laser light and hence restricted to transparent vessels. However, with the penetrative power of x rays, the brilliant intensities achievable at synchrotron facilities and ever-improving ultrafast detector systems, these restrictions are overcome. While several important advances in the field of x-ray PIV have been made via the study of microparticles seeded within a fluid mix,^{6,7} remarkably with blood it is possible to achieve contrast without the addition of any marker. Propagation-based phase contrast⁸ is obtained in the form of a characteristic speckle pattern^{5,9} caused by the lensing and interference of the weakly scattered wavefield, which results from propagation through numerous red blood cells (RBCs) (typical hematocrit, or volume density is $\sim 45\%$). This use of phase contrast is necessary, as the mass density difference between the cells and their surrounding plasma matrix is less than 10%, and consequently the contrast of purely absorption-based imaging is insufficient to visualize blood flow.

The usefulness of phase-contrast imaging systems for extracting both quantitative and qualitative sample information is well established, particularly in biomedical applications (see, for example, the review article by Momose¹⁰). In this letter, we demonstrate the benefits to be gained by the application of a simple phase retrieval algorithm to the speckled propagation-based phase-contrast images used for x-ray PIV analysis. The improved correlation-peak forms re-

veal information over the entire depth, which is then used to tomographically reconstruct the radially varying velocity profile. Unlike the complementary technique of particle tracking velocimetry,⁷ which requires the ability to individually identify particles in at least two imaging frames, this statistically robust three-dimensional measurement is applicable to speckled images with no upper limit of particle seeding density within the sample.

The *in vitro* experiment was conducted on the 20XU undulator beamline at the SPring-8 synchrotron, Japan. We worked at the upstream hutch, located 80 m from the source ($\sim 10^{13}$ photons/mm²/s). A schematic of the experimental configuration is shown in Fig. 1. X-ray energies of 25 keV were selected with a Si-111 monochromator. The sample was a cylindrical glass capillary of 570 μm inner diameter and 200 μm wall thickness, through which a porcine blood mixture was pumped by a Harvard microsyringe pump system. Maximum visibility of speckle was achieved at a sample-to-detector propagation distance of 38 cm.

Blood, with the plasma replaced by an equal amount of higher-density sucrose solution, was used to reduce separation. A 50 \times magnification lens was used with a phosphor beam monitor and PCO 4000 charge coupled device camera, such that the effective pixel size was 0.19 μm . Power-spectrum analysis yields an uppermost real spatial frequency corresponding to 1.1 μm . Exposures of 20 ms were taken at a rate of 2 s⁻¹. A synchronized shutter system was implemented to prevent unnecessary exposure between each frame.

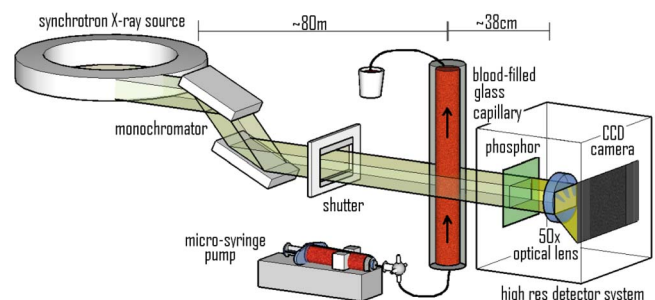


FIG. 1. (Color online) Schematic of x-ray phase-contrast PIV experiment.

^{a)}Electronic mail: sally.irvine@sci.monash.edu.au.

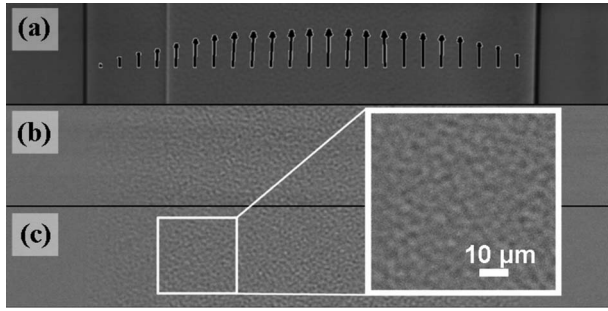


FIG. 2. Set of x-ray phase-contrast images of flowing blood contained within cylindrical vessel. (a) Raw image (vertical white line formed by a ridge on outside of tube) with superimposed velocimetric profile, showing minimum flow velocities at the wall and maximum in the center. (b) Average-subtracted image. (c) Average-subtracted image after Fourier mask filtering. Magnified inset demonstrates characteristic speckled interference pattern constituting the signal used for PIV.

Prior to PIV analysis, preprocessing of the images (standard in the context of quantitative x-ray phase retrieval, see, e.g., Gureyev *et al.*¹¹) significantly increased the signal-to-noise ratio. The first step was the average subtraction of the images, taking the average from a distant part of the image sequence in order to prevent bias against very slow moving particles. The images were then Fourier mask filtered to remove the regular streaks caused by the monochromator, taking care not to eliminate those spatial frequencies prominent in the speckle pattern (Fig. 2).

A single-image phase retrieval method was then applied to the images. An expression for the reconstructed projected thickness is derived by Paganin *et al.*,¹² and due to the weakness of absorption and significant levels of noise, we make use of a Tikhonov regularization parameter¹³ (recently employed in Groso *et al.*¹⁴ and Friis *et al.*¹⁵). The following equation for the projected thickness $T(\mathbf{r}_\perp, \lambda)$ then applies¹²

$$T(\mathbf{r}_\perp, \lambda) = - (1/\mu) \ln \mathbf{F}^{-1} \left\{ \frac{(\mu/I_0) \mathbf{F}[I(\mathbf{r}_\perp, \lambda)]}{\mu + z \delta \mathbf{k}_\perp^2 + \varepsilon} \right\}, \quad (1)$$

where \mathbf{F} denotes Fourier transformation, \mathbf{k}_\perp denotes the spatial frequencies dual to transverse spatial coordinates \mathbf{r}_\perp , and ε is a regularization parameter that is inversely proportional to the signal-to-noise ratio. For a two-component sample, such as represented by RBCs inside the plasma matrix, μ and δ are given by the difference between refractive indices of the two materials.¹¹ The denominator describes a low-pass band filter. ε is determined by inspection of both the images themselves (the filter's amplification of low-frequency noise is well documented)¹⁶ and the cross-correlation peaks of consecutive images.

For the latter, each image was segmented into multiple interrogation windows 256×256 pixels in area. We are reminded of the difference between conventional PIV and x-ray phase-contrast PIV by the form of the cross-correlation peaks. The term *particle* imaging is misleading here as we are in fact only indirectly measuring the particle (RBC) displacement from the consequent variation in the interference pattern. At high spatial resolution, the cross-correlation peaks of the speckle images reveal what the eye cannot see, that is, at least one strong diffraction-induced ring around the central peak of intensity *below* the noise skirt. This ring in the correlation function and the accompanying oscillations is a signature of propagation-based phase contrast.⁸ Phase retrieval

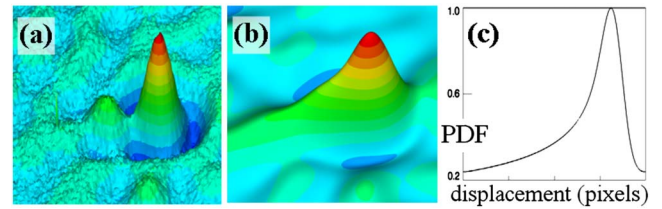


FIG. 3. (Color online) Cross-correlation peaks (a) before and (b) after the application of phase retrieval. The relevant region of the full interrogation window has been magnified for clarity. In (c), the theoretical PDF for parabolic flow of finite sized particles is shown for comparison.

decodes the image contrast to remove the effects of Fresnel diffraction.⁸ The reconstruction algorithm is applied with a suitably chosen regularization parameter, tuned such that the ring in the correlation function just disappears (cf. Paganin *et al.*¹³). Figure 3 shows the cross-correlation peaks for an interrogation region at the capillary center, both before [Fig. 3(a)] and after [Fig. 3(b)] phase retrieval. In addition to significantly reducing the noise in the correlation, phase retrieval yields substantially better definition of the peak profile.

After the phase retrieval, standard PIV may be applied to optimally measure the most likely particle displacement for each interrogation region. The resulting velocity profile across the vessel diameter represents only the modal velocity and as such is not a three-dimensional measurement since it does not take into account the out-of-image-plane variation in flow. For a more complete measurement, we use the fact that each cross-correlation peak represents a probability density function (PDF) of the velocity within the measurement volume.⁶ This is clearly demonstrated in Fig. 3(c), which shows the theoretical peak formed by the convolution of a PDF with a Gaussian function whose full width at half maximum corresponds to twice the finite particle width. From the PDF we may derive the expected value, or average velocity within the volume. Integration yields the projected velocity. If we assume axial flow symmetry consistent with a cylindrical geometry, a simple tomographic reconstruction of the radial profile (based on the inverse Abel transform) is possible. We used a sixth-order even polynomial to fit to the projected velocity. Note that we do not regard the time-smearing of the peaks as significant: the exposure-to-interframe time ratio of 20 to 500 ms is small and as such, the increased accuracy to be gained through a Richardson-type extrapolation may be assumed negligible.⁶

Figure 4(a) shows the projected velocity (i.e., the line integral of velocities along the direction of propagation) directly calculated from the cross-correlation peaks after phase retrieval. At ε values close to the optimal, the result is somewhat insensitive to ε ; we have used $\varepsilon = 800 \mu$. Figure 4(b)

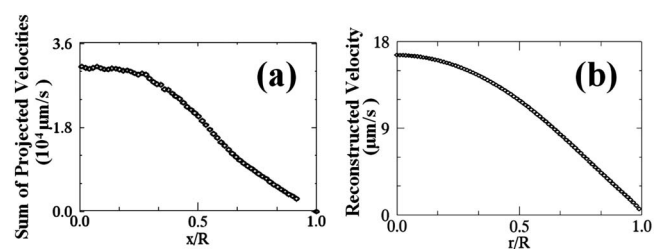


FIG. 4. (a) Sum of velocities through projection (calculated directly from cross-correlation peak integral) and (b) reconstructed radial velocity profile.

shows the final reconstructed radial velocity profile. The shape and magnitude of the profile is consistent with the expected Poiseuille circular pipe flow. We note that while the velocity is slightly greater than zero at the radius corresponding to the capillary wall, this is thought to be a direct result of the finite interrogation window size.

In conclusion, we have demonstrated the usefulness of phase retrieval as a method for the improvement of high-resolution phase-contrast images for PIV flow measurement. In addition, we have obtained a three-dimensional velocity measurement from a single-image x-ray phase-contrast sequence in reconstructing the radial flow profile of blood flowing through a cylindrical capillary tube.

The authors acknowledge the Japan Synchrotron Radiation Research Institute (Proposal No. 2007B1329), the Access to Major Research Facilities Program, and the Australian Research Council. S.C.I. is a recipient of an Australian Postgraduate Award.

¹E. Boersma, N. Mercado, D. Poldermans, M. Gardien, J. Vos, and M. L. Simoons, *Lancet* **361**, 847 (2003).

- ²S. A. Berger and L. D. Jou, *Annu. Rev. Fluid Mech.* **32**, 347 (2000).
³D. J. Dowsett, P. A. Kenny, and R. E. Johnston, *Physics of Diagnostic Imaging* (Chapman and Hall, London, 1998).
⁴S. J. Lee and G. B. Kim, *J. Appl. Phys.* **94**, 3620 (2003).
⁵G. B. Kim and S. J. Lee, *Exp. Fluids* **41**, 195 (2006).
⁶A. Fouras, J. Dusting, R. Lewis, and K. Hourigan, *J. Appl. Phys.* **102**, 064916 (2007).
⁷K.-S. Im, K. Fezzaa, Y. J. Wang, X. Liu, J. Wang, and M. C. Lai, *Appl. Phys. Lett.* **90**, 091919 (2007).
⁸D. M. Paganin, *Coherent X-Ray Optics* (Oxford University Press, Oxford, 2006).
⁹M. J. Kitchen, D. Paganin, R. A. Lewis, N. Yagi, K. Uesugi, and S. T. Mudie, *Phys. Med. Biol.* **49**, 4335 (2004).
¹⁰A. Momose, *Jpn. J. Appl. Phys., Part 1* **44**, 6355 (2005).
¹¹T. E. Gureyev, A. W. Stevenson, D. M. Paganin, T. Weitkamp, A. Snigirev, I. Snigireva, and S. W. Wilkins, *J. Synchrotron Radiat.* **9**, 148 (2002).
¹²D. Paganin, S. C. Mayo, T. E. Gureyev, P. R. Miller, and S. W. Wilkins, *J. Microsc.* **206**, 33 (2002).
¹³D. Paganin, T. E. Gureyev, K. M. Pavlov, R. A. Lewis, and M. Kitchen, *Opt. Commun.* **234**, 87 (2004).
¹⁴A. Groso, R. Abela, and M. Stampanoni, *Opt. Express* **14**, 8103 (2006).
¹⁵E. M. Friis, P. R. Crane, K. R. Pedersen, S. Bengtson, P. C. J. Donoghue, G. W. Grimm, and M. Stampanoni, *Nature (London)* **450**, 549 (2007).
¹⁶D. Paganin, A. Barty, P. J. McMahon, and K. A. Nugent, *J. Microsc.* **214**, 51 (2004).